Center for Turbulence Research
Proceedings of the Summer Program 1994

Pressure and higher-order spectra for homogeneous isotropic turbulence

By D. I. Pullin[1] AND R. S. Rogallo[2]

The spectra of the pressure, and other higher-order quantities including the dissipation, the enstrophy, and the square of the longitudinal velocity derivative are computed using data obtained from direct numerical simulation of homogeneous isotropic turbulence at Taylor-Reynolds numbers R_λ in the range $38 - 170$. For the pressure spectra we find reasonable collapse in the dissipation range (of the velocity spectrum) when scaled in Kolmogorov variables and some evidence, which is not conclusive, for the existence of a $k^{-7/3}$ inertial range, where $k = |\mathbf{k}|$ is the modulus of the wavenumber. The power spectra of the dissipation, the enstrophy, and the square of the longitudinal velocity derivative separate in the dissipation range, but appear to converge together in the short inertial range of the simulations. A least-squares curve-fit in the dissipation range for one value of $R_\lambda = 96$ gives a form for the spectrum of the dissipation as $k^0 \exp(-Ck\eta)$, for $k\eta > 0.2$, where η is the Kolmogorov length and $C \approx 2.5$.

1. Introduction

The collapse of data for the various forms of the velocity power spectrum when scaled in Kolmogorov variables of the form

$$E(k) = (\nu^5\langle\varepsilon\rangle)^{1/4} f_1(k\eta), \tag{1}$$

is well established as either an exact, or at least a very good approximation at large Reynolds numbers, by both experiment and numerical simulation; see for example Saddoughi & Veeravalli (1994) for an update of a graphical compilation originally due to Chapman (1979). In (1) E is either the shell-summed spectrum or a form of the related one-dimensional spectra, $\eta = (\nu^3/\langle\varepsilon\rangle)^{1/4}$ is the Kolmogorov length, and $\langle\varepsilon\rangle$ is the volume-averaged dissipation. The aim of the present work is to use numerical data bases obtained from direct numerical simulation (DNS) of homogeneous isotropic turbulence to study the power spectra of several quantities that are quadratic in the velocity or its spatial derivative. It is hoped that the results may be useful for testing the predictive capability of theories or models of turbulent fine scales as well as adding to our basic understanding of turbulence in the inertial and dissipation ranges.

1 Graduate Aeronautical Laboratory, California Institute of Technology, Pasadena CA 91125
2 NASA Ames Research Center

We shall consider two-point correlations and associated power spectra of quantities that are scalar functions of position in homogeneous isotropic turbulence. Let $q(\mathbf{x},t)$ be an arbitrary function of position $\mathbf{x} \equiv (x_1, x_2, x_3)$ and time t, and denote its Fourier transform by

$$\hat{q}(\mathbf{k}) = \frac{1}{8\pi^3} \int\int\int q(\mathbf{x}) \mathrm{e}^{-\mathrm{i}\mathbf{k}\cdot\mathbf{x}} \, d\mathbf{x}. \tag{2}$$

In (2) and subsequently we have suppressed the explicit dependence on t. Define the two-point one-time correlation of $q(\mathbf{x})$ at points $\mathbf{x}$, $\mathbf{x}+\mathbf{r}$ by

$$Q(\mathbf{r}) = \langle q(\mathbf{x}) q(\mathbf{x}+\mathbf{r}) \rangle, \tag{3}$$

where $\langle ... \rangle$ is a volume average over $\mathbf{x}$. The Fourier transform of $Q(\mathbf{r})$ is

$$\Pi(\mathbf{k}) = \frac{1}{8\pi^3} \int\int\int Q(\mathbf{r}) \mathrm{e}^{-\mathrm{i}\mathbf{k}\cdot\mathbf{r}} \, d\mathbf{r}, \tag{4}$$

and it is easy to show that

$$\Pi(\mathbf{k}) = \hat{q}(\mathbf{k}) \hat{q}^*(\mathbf{k}), \tag{5}$$

where $*$ denotes the complex conjugate. On integrating (5) over the surface of a sphere $S(\mathbf{k})$ of radius k in $\mathbf{k}$-space, we obtain

$$E_q(k) = \int\int_{S(\mathbf{k})} \Pi(\mathbf{k}) \, dS(\mathbf{k}). \tag{6}$$

We shall refer to $\hat{q}(\mathbf{k})\hat{q}^*(\mathbf{k})$ as the power spectrum of $q(\mathbf{x})$ and to $E_q(k)$ defined by (6) as its shell-summed power spectrum. When the turbulence is isotropic and $q(\mathbf{x})$ is an invariant scalar in the sense that its value at any point is axis independent, then $Q(\mathbf{r}) = Q(r)$, $r = |\mathbf{r}|$, and $\Pi(\mathbf{k}) = \Pi(k)$, $k = |\mathbf{k}|$. The right-hand side of (6) is then equal to $4\pi k^2 \Pi(k)$.

We consider power spectra of four quantities for which $q(\mathbf{x})$ is identified in turn with the following: the pressure-density ratio $p(\mathbf{x})$, the dissipation $\varepsilon = 2\nu(\partial u_i/\partial x_j + \partial u_j/\partial x_i)^2$, the enstrophy density $\Omega = \boldsymbol{\omega}^2$, and a quantity proportional to the square of the longitudinal velocity derivative $\Upsilon = 15(\partial u)^2$, where $\partial u \equiv \partial u_1/\partial x_1$ and $\mathbf{u} = (u_1, u_2, u_3)$ is the velocity vector. We denote the shell-summed power spectra of these quantities, in Kolmogorov scaling variables, respectively by

$$E_p(k) = \langle\varepsilon\rangle^{3/4} \nu^{7/4} f_2(k\eta), \tag{7}$$

$$E_\varepsilon(k) = \langle\varepsilon\rangle^{7/4} \nu^{3/4} f_3(k\eta), \tag{8}$$

$$E_\Omega(k) = \langle\varepsilon\rangle^{7/4} \nu^{-5/4} f_4(k\eta), \tag{9}$$

$$E_\Upsilon(k) = \langle\varepsilon\rangle^{7/4} \nu^{-5/4} f_5(k\eta). \tag{10}$$

For homogeneous isotropic turbulence, $\langle\varepsilon\rangle$, $\langle\Omega\rangle$, and $\langle\Upsilon\rangle$ are nonzero and satisfy the relations

$$\langle\varepsilon\rangle = \nu\langle\Omega\rangle = \nu\langle\Upsilon\rangle. \tag{11}$$

In (8-10) these mean values are subtracted, and the integrals of the right-hand sides over $k = (0, \infty)$ are equal to the fluctuations, respectively, $\left\langle\epsilon'^2\right\rangle \equiv \langle(\varepsilon - \langle\varepsilon\rangle)^2\rangle$, $\left\langle\Omega'^2\right\rangle \equiv \langle(\Omega - \langle\Omega\rangle)^2\rangle$, and $\left\langle\Upsilon'^2\right\rangle \equiv \langle(\Upsilon - \langle\Upsilon\rangle)^2\rangle$.

We remark that $(\partial u_1/\partial x_1)^2$ is not a proper scalar, but is one component of the fourth-order tensor

$$\left(\frac{\partial u_i}{\partial x_j}\right)\left(\frac{\partial u_l}{\partial x_m}\right)$$

whose two-point correlation is an eighth-order tensor. As a consequence the power spectrum of Υ is not uniform over spherical surfaces in **k**-space. We nevertheless treat Υ as if it were a scalar for the reason that it has been used as a surrogate for ε in experiment, being the gradient-variance that can most easily be measured with a hot-wire probe. It is therefore of interest to compare its fluctuations with those of ε and Ω. Note that (3-5) remain valid and (6) may still be applied.

2. Data bases

For the most part we have used data from the forced DNS runs of Jiménez *et al.* (1993), henceforth referred to as *JWSR*. See their §2 for a detailed description of the numerical experiments and their Table 1 for a summary of the flow parameters. Our data base differs from *JWSR* Table 1 as follows: first, *JWSR* take both volume and time averages, the latter being over several large-eddy turnover times, whereas our results are based on Fourier coefficients of the velocity from a single time frame, being the last for the run. Comparisons made with one-time results at earlier times separated by a substantial fraction of a large-eddy turnover time indicated that statistical equilibrium had been obtained. Because we are using a single time frame our values $R_\lambda = 38\,(64^3)$, $65\,(128^3)$, $96\,(256^3)$, and $170\,(256^3)$ (the bracketed number gives the numerical grid resolution N^3) differ slightly from those of *JWSR*. Secondly and more importantly, our largest R_λ run was at a resolution of 256^3 compared to the 512^3 run of *JWSR* which was unavailable to us. Since the 256^3 data at $R_\lambda = 170$ has $k_{max}\eta \approx 1.0$ compared with $k_{max}\eta \approx 2.0$ for all the *JWSR* runs, it may be somewhat under-resolved. All shell-summed spectra were calculated directly from coefficients in **k**-space with de-aliased quadratic products evaluated in physical space. Those for the pressure were obtained from a solution of the relevant Poisson equation.

For the pressure spectra, in addition to the DNS runs, we also consider results from two kinds of LES (large-eddy simulation) runs. The first of these utilizes a method in which, at every time step, the magnitudes of the Fourier components of the velocity are adjusted, with no change to either the relative magnitudes in the (x_1, x_2, x_3) directions or the complex phases, such that the velocity spectrum was locked to a $k^{-5/3}$ form. We will refer to this as *Locked-E* LES (She & Jackson,

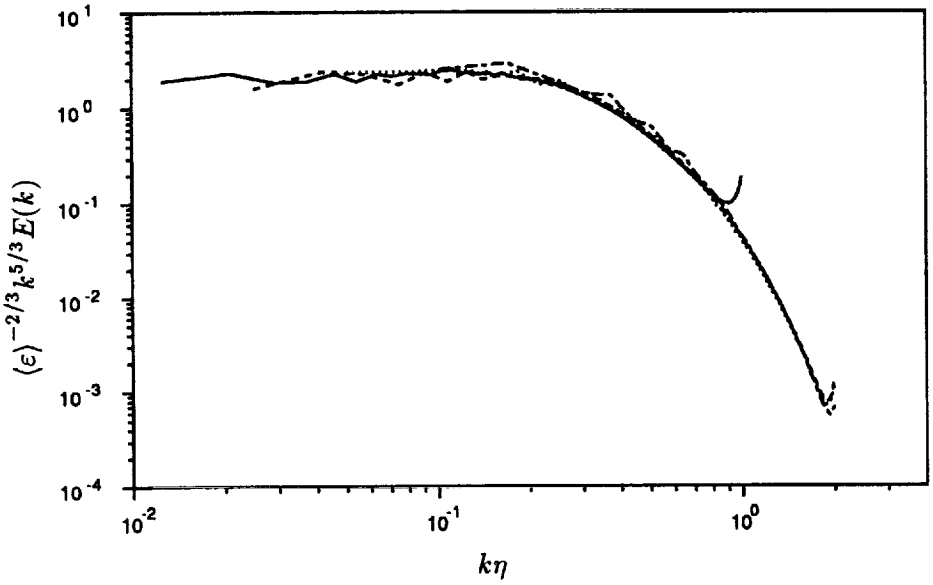

FIGURE 1. Compensated velocity power spectra in Kolmogorov units. —— $R_\lambda = 170$, ---- $R_\lambda = 96$, ····· $R_\lambda = 65$, —·— $R_\lambda = 38$.

1993). In addition some pressure spectra calculated from a Smagorinsky subgrid approach using the so called *dynamic localization model* (*DLM*, Ghosal *et al.* 1994) are also presented.

3. Spectrum of the pressure

Fig. 1 shows the velocity (energy) spectrum plotted in the compensated inertial-range form $\langle\varepsilon\rangle^{-2/3}k^{5/3}E(k) = (k\eta)^{5/3}f_1(k\eta)$. The data, including the $R_\lambda = 170$ case, collapses reasonably across the whole range of $k\eta$. A Kolmogorov constant of $\mathcal{K}_0 \approx 2.2$ appears to be indicated, but as pointed out by Jiménez (private communication), the plateau at $k\eta < 0.2$ may in fact be part of a bump in the spectrum near the beginning of the dissipation range (see Saddoughi & Veeravalli, 1994, for related experimental evidence), which is not properly resolved owing to the small inertial range of the DNS. The above quoted $\mathcal{K}_0$ may then be an overestimate.

It is well known that Kolmogorov-type dimensional arguments suggest a form for E_p in the inertial range

$$E_p(k) = \mathcal{K}_p \langle\varepsilon\rangle^{4/3} k^{-7/3}, \tag{12}$$

where $\mathcal{K}_p$ is a dimensionless number which may or may not be a universal constant. In Fig. 2 $E_p(k)$ is plotted in the compensated form suggested by (12), $\langle\varepsilon\rangle^{-4/3}k^{7/3}E_p(k) = (k\eta)^{7/3}f_2(k\eta)$. The collapse in the dissipation range (by which we mean $k\eta$ greater than about 0.125) is only fair if one discards the $R_\lambda = 170$ case as under-resolved, and poor if it is included. If this case is discarded Fig. 2 is consistent with a possible plateau corresponding to $\mathcal{K}_p \approx 8.5$, which is somewhat higher than the value $\mathcal{K}_p \approx 7$ suggested by Pumir (1994). Again, owing to the small

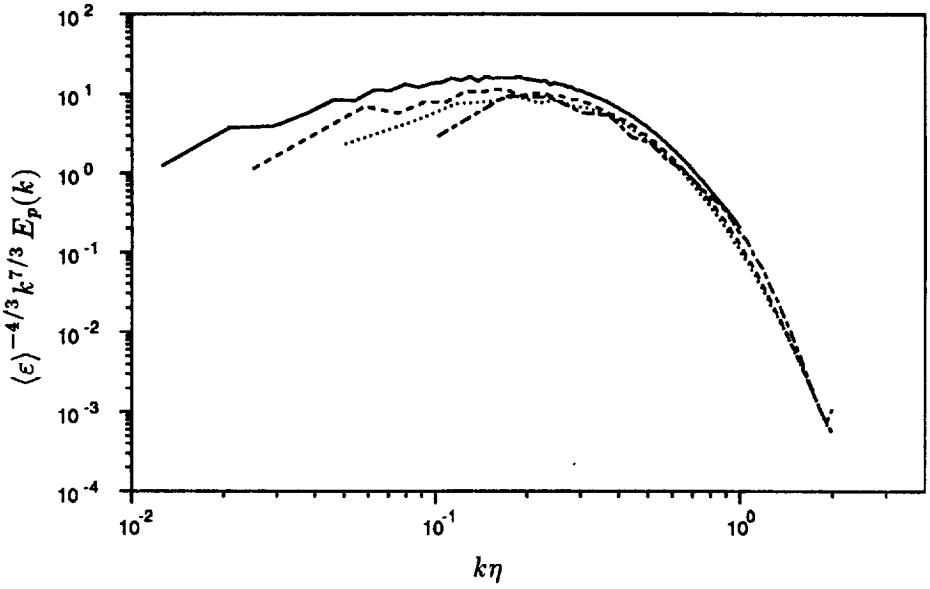

FIGURE 2. Compensated pressure spectra in Kolmogorov units. —— $R_\lambda = 170$, ---- $R_\lambda = 96$, ····· $R_\lambda = 65$, —·— $R_\lambda = 38$.

inertial range, definitive conclusions cannot be drawn and we cannot rule out the possibility of a bump analogous to that found found for $E(k)$ with or without a plateau at lower $k\eta$.

An argument due to Obukov (1949) and Batchelor (1951) based on a joint-normal hypothesis for the two-point probability distribution of the velocity field suggests that $\mathcal{K}_0$ and $\mathcal{K}_p$ (if they exist) are related as

$$\mathcal{K}_p = \frac{4536\,\left(\Gamma\left[\frac{4}{3}\right]\right)^2}{3025\,\Gamma\left[\frac{5}{3}\right]}\mathcal{K}_0^2 = 1.3245105..\mathcal{K}_0^2. \tag{13}$$

Taking $\mathcal{K}_0 = 1.5$ gives, from (13), $\mathcal{K}_p = 2.98$ which is much lower than the peak shown in Fig. 2 but which agrees approximately with the range of values $2.4 - 3.4$ estimated by Pullin (1994) from the Lundgren (1982) stretched spiral vortex model.

The ratio $E_p(k)/(k\,E(k)^2)$ is shown in Figs. 3-4. If both $E(k)$ and $E_p(k)$ follow their respective K-41 power laws in the inertial range, this ratio should plateau at $\mathcal{K}_p/\mathcal{K}_0^2$. As a test of our means of calculating E_p, the phases of the Fourier coefficients of the velocity field for the *Locked-E* LES run were randomized without change to their magnitudes. This should produce a Gaussian joint-normal velocity probability distribution while maintaining a $k^{-5/3}$ inertial range. The plateau shown in Fig. 3 for this case is in good agreement with (13) as indeed it should be (see the article by Gotoh & Rogallo in these proceedings for a discussion of various spectra for Gaussian velocity pdf's). The roll-off at both large and small k is attributed to the finite range of k in the calculation of the pressure via the (elliptic) Poisson equation, which evidently "feels" the bounded dimensions of the box. The

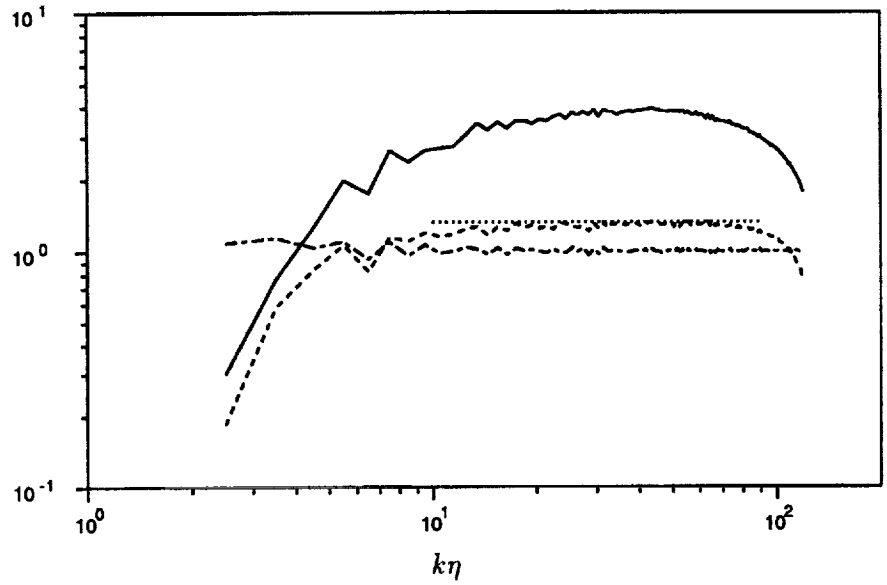

FIGURE 3. Deviation of the pressure spectrum in an inertial range from the joint-normal theory. ——— , $k^{5/3}E(k)$; —— $E_p(k)/(k\,E(k)^2)$ from 256^3 *Locked-E* LES. ---- $E_p(k)/(k\,E(k)^2)$ from 256^3 joint-normal velocity field. ····· equation 13.

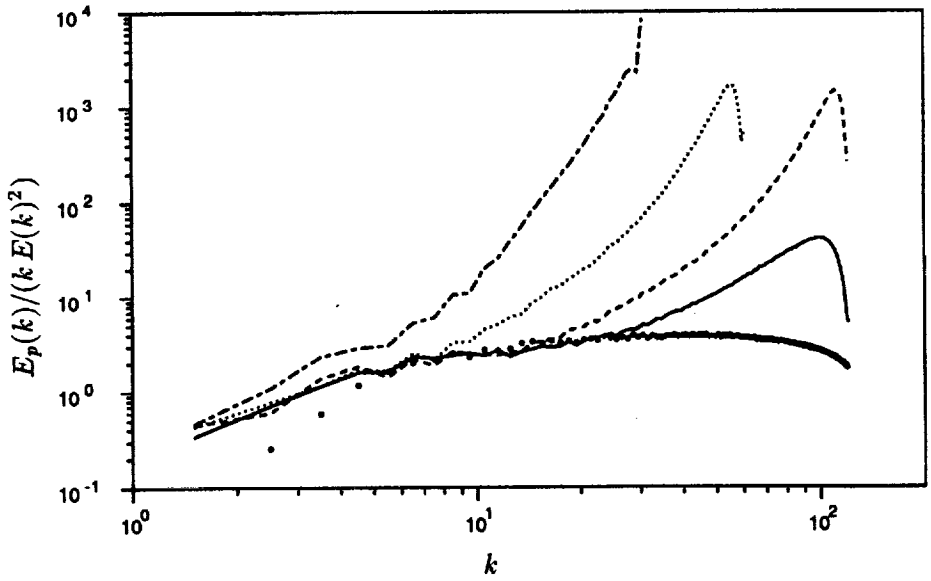

FIGURE 4. Variation of $E_p(k)/(k\,E(k)^2)$ with Reynolds number. —— $R_\lambda = 170$, ---- $R_\lambda = 96$, ····· $R_\lambda = 65$, ——— $R_\lambda = 38$. • 256^3 *Locked-E* LES.

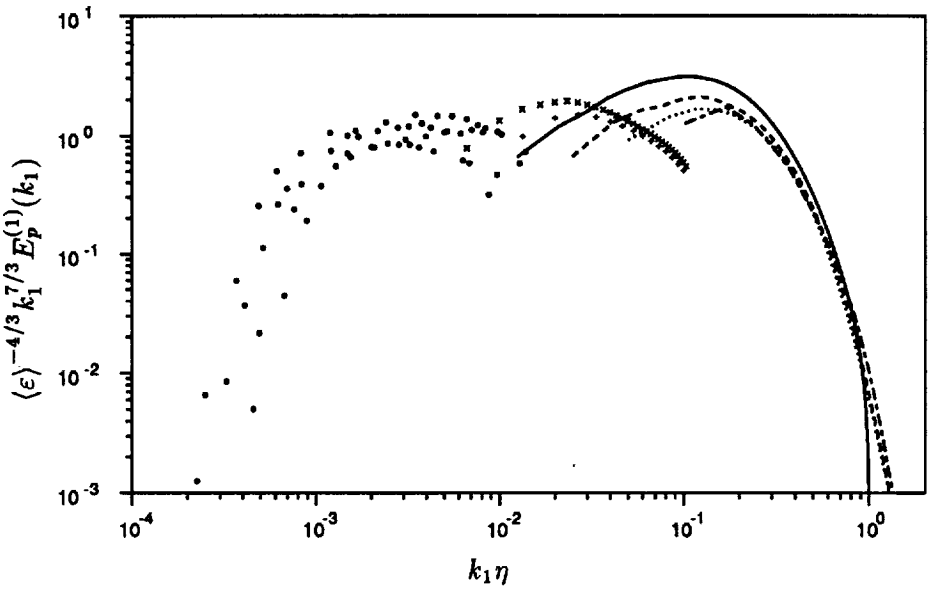

FIGURE 5. Compensated one-dimensional pressure spectra in Kolmogorov units. —— $R_\lambda = 170$, ---- $R_\lambda = 96$, ····· $R_\lambda = 65$, —·— $R_\lambda = 38$. × *DLM* LES (64^3), $R_\lambda = 269$. + *DLM* LES (32^3), $R_\lambda = 176$. • experiment of George *et al.* (1984).

true *Locked-E* LES also shows a plateau in Figs. 3-4, but at a value close to 3.8. In Fig. 4 the DNS and *Locked-E* LES show agreement in a small range of k at the larger R_λ.

An attempt to bring experiment, DNS, and LES results together is made in Fig. 5 which plots the one-dimensional form of the pressure spectrum

$$E_p^{(1)}(k_1) = \frac{1}{2}\int_{k_1}^{\infty} \frac{1}{\kappa'} E_p(\kappa')\, d\kappa'. \tag{14}$$

The measurements of George *et al.* (1984) shown in Fig. 5 were made in the mixing layer of a turbulent jet at 1.5 – 3 diameters downstream of the jet exit. Reynolds numbers based on the exit velocity and jet diameter were 4.0×10^5 and 6.2×10^5. Taylor Reynolds numbers were in the range $R_\lambda \approx 350 - 600$. George *et al.* nondimensionalized their data with large-scale parameters which may be more appropriate at the fairly low wavenumbers of the experiment. We have rescaled their results using estimates of the dissipation and of the Kolmogorov microscale given in §17 of their paper. They state that velocity contamination caused by flow-probe interactions may have had some effect on the accuracy of the data. Fig. 5 well illustrates the difficulties of studying pressure correlations. Neither DNS, which is currently limited to low R_λ, nor experiment, which is limited by accuracy problems at large wavenumbers, can span an appreciable spectral band. The combined experiment, *DLM* LES, and DNS results may indicate a plateau in

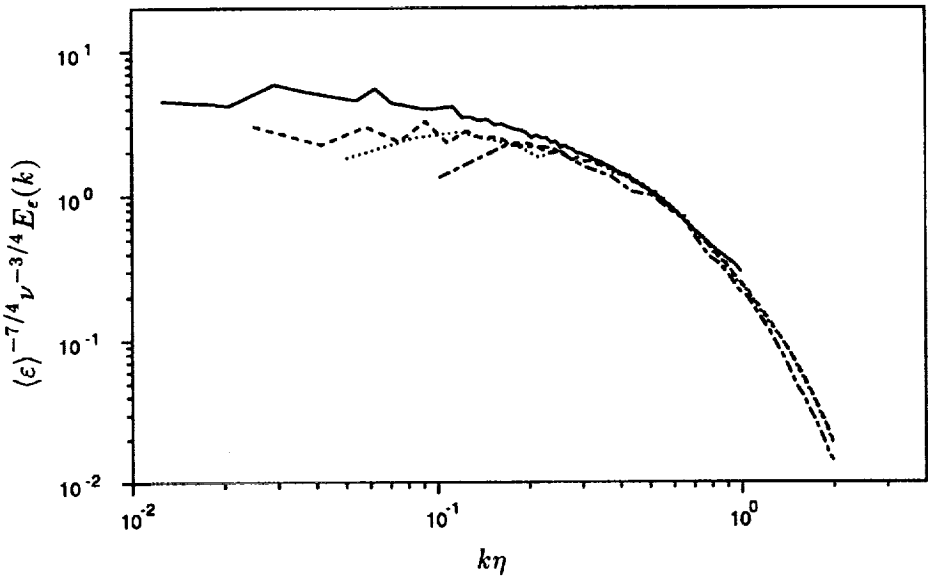

FIGURE 6. Power spectra of the dissipation in Kolmogorov units. —— $R_\lambda = 170$, ---- $R_\lambda = 96$, ····· $R_\lambda = 65$, —·— $R_\lambda = 38$.

the $k_1^{7/3}$-compensated spectra, but the scatter is very large. If (12) is true then from (14) the one-dimensional inertial-range coefficient is $\mathcal{K}_p^{(1)} = \frac{3}{14}\mathcal{K}_p$.

4. Spectra of ϵ, Ω, and Υ

Calculated dissipation spectra E_ϵ and enstrophy spectra E_Ω are shown in Figs. 6 and 7 respectively. Fig. 8 shows a comparison of these together with the spectrum of $\Upsilon = 15(\partial u_1/\partial x_1)^2$ at $R_\lambda = 96$. This indicates that the fluctuations of Ω are rather larger than those of ε/ν with fluctuations of $15(\partial u_1/\partial x_1)^2$ larger still. If Kolmogorov scaling is exact then the quantities $\langle\varepsilon^2\rangle/\langle\varepsilon\rangle^2$, $\langle\Omega^2\rangle/\langle\Omega\rangle^2$, and $\langle(\partial u)^4\rangle/\langle(\partial u)\rangle^2$ should each be constant independent of Reynolds number. There is evidence from DNS, *e.g.* Kerr (1985), *JWSR*, that this is not the case for $\langle(\partial u)^4\rangle/\langle(\partial u)\rangle^2$, which exhibits a weak dependence on the Taylor Reynolds number $R_\lambda = u\lambda/\nu$, where u is the root-mean square of one component of the velocity and λ is the Taylor microscale. This is confirmed by Gotoh & Rogallo in these proceedings who also tabulate $\langle\varepsilon^2\rangle/\langle\varepsilon\rangle^2$, $\langle\Omega^2\rangle/\langle\Omega\rangle^2$ for the present data set.

It is notable that Fig. 8 shows no sign of power-law behavior at low k, and indeed an asymptote to a constant appears to be indicated for all three quantities. This is in qualitative agreement with measurements, made using a multi-wire probe, of Tsinober *et al.* (1992) (see their Fig. 9(a)). In Fig. 9 we have plotted the spectra of Fig. 8 in the form $d[\log(f_n(k\eta))]/d[\log(k\eta)]$, $n = 3,4,5$ where f_n are defined by Equations (8-10). If curves are of the form $(k\eta)^\beta \exp(-Ck\eta)$, then this plot should be a straight line of slope $-C$ that intercepts the vertical axis at β. The fit of a

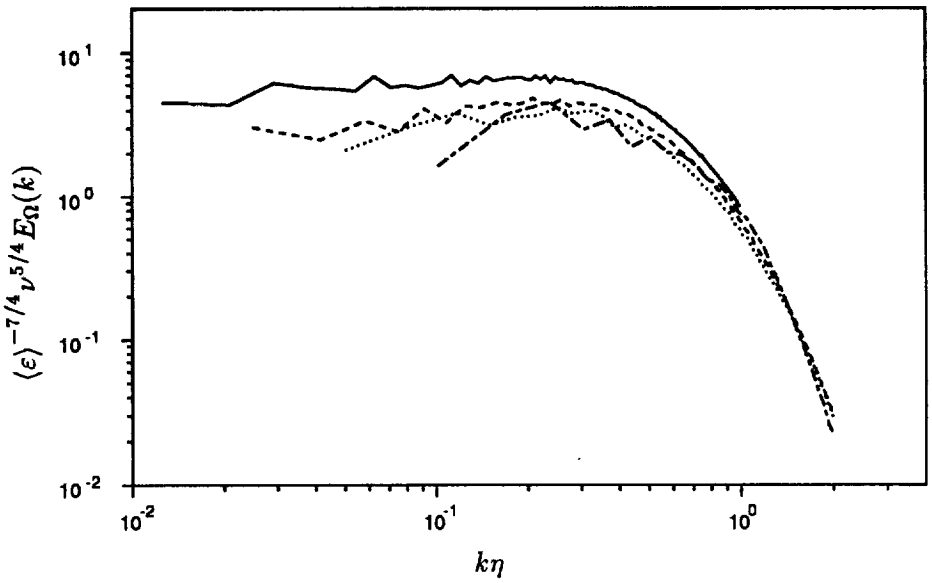

FIGURE 7. Power spectra of the enstrophy in Kolmogorov units. —— $R_\lambda = 170$, ---- $R_\lambda = 96$, ····· $R_\lambda = 65$, —·— $R_\lambda = 38$.

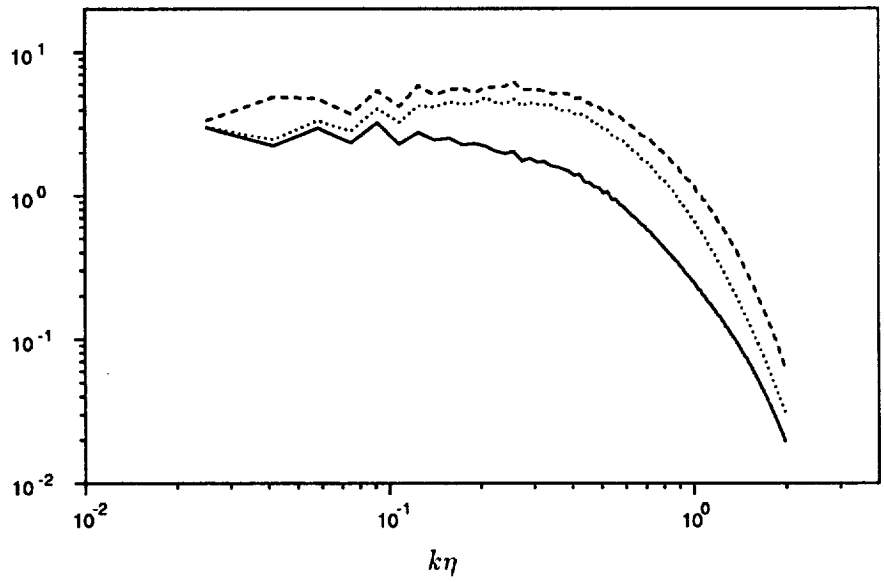

FIGURE 8. Comparison of quadratic velocity-derivative spectra at $R_\lambda = 96$. —— ϵ, ····· Ω, ---- $\Upsilon = 15(\partial u_1/\partial x_1)^2$.

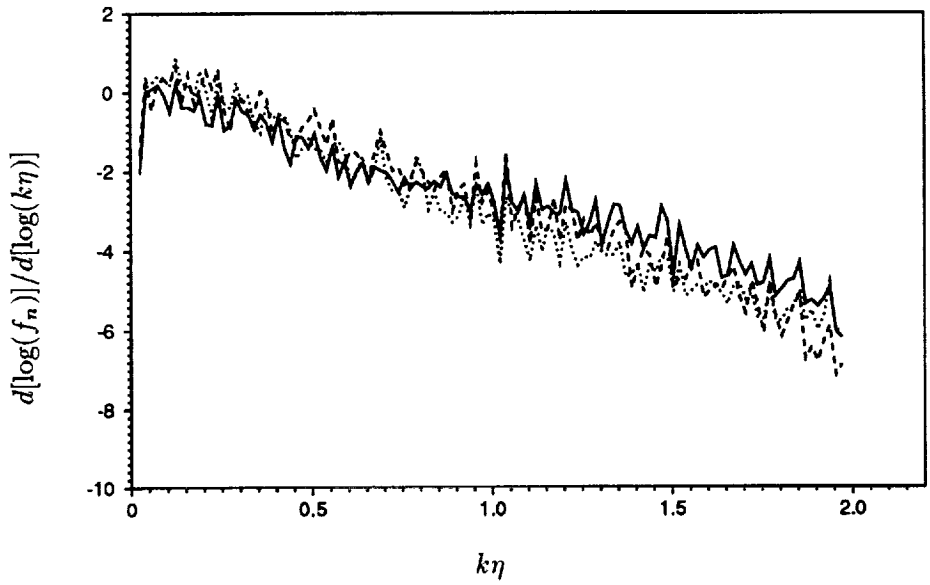

FIGURE 9. Spectra of Fig. 8 plotted in the form $d[\log(f_n(k\eta))]/d[\log(k\eta)]$, $n = 3,4,5$ where f_n are defined by Equations (8-10). —— ϵ, ····· Ω, ---- $\Upsilon = 15(\partial u_1/\partial x_1)^2$.

straight line to the data sets in Fig. 9 is very approximate. Nevertheless a least-squares best fit was made in each case in the window $0.2 < k < 1.8$. The method was tested using the velocity spectrum (not shown) for which we found $\beta = -1.6$ and $C = 4.9$ in fair agreement with Kerr (1990) and others. We find that for E_ϵ; $\beta \approx 0.$, $C \approx 2.5$, E_Ω; $\beta \approx 0.5$, $C \approx 3.5$. There was some sensitivity to the chosen range, so the errors are substantial, of order ± 0.1 for β and ± 0.2 for C. Clearly a larger resolved dissipation range is needed to improve accuracy.

5. Concluding remarks

We have examined the power spectra of several quantities using numerical data bases from DNS and LES box turbulence, focusing mainly on flow variables that are quadratic in the velocity components and which have proven difficult to measure experimentally. When taken in conjunction with the one-dimensional spectra of Figure 5, the DNS shell-summed spectra provide tentative evidence for the presence of a $k^{-7/3}$ range with $\mathcal{K}_p \approx 8.5$ and a corresponding $\mathcal{K}_p^{(1)} \approx 1.8$, but with large error. These are higher than those predicted by either the joint-Gaussian model ($\mathcal{K}_p \approx 2.98$ corresponding to $\mathcal{K}_0 = 1.5$) or the stretched-spiral vortex model ($\mathcal{K}_p = 2.4 - 3.4$ depending on R_λ). Since it is unlikely that the spectral range of DNS will increase sufficiently in the near future to resolve this issue, there is clearly a need for a definitive experiment of the Saddoughi & Veeravalli (1994) type. The spectra of $\langle\varepsilon\rangle$ and $\langle\Omega\rangle$ show significant differences in the dissipation range but appear to behave similarly in the short inertial range, where a k^0 form is indicated, in agreement with the prediction of the stretched spiral-vortex model (Pullin *et al.* 1994).

Acknowledgments

The authors wish to thank T. Gotoh for helpful discussions. DIP was partially supported under NSF Grant CTS-9311811. Hospitality provided by CTR during the 1994 Summer Research Program is gratefully acknowledged.

REFERENCES

BATCHELOR, G. K. 1951 Pressure fluctuations in isotropic turbulence. *Proc. Camb. Phil. Soc.* **47**, 359-374.

CHAPMAN, D. 1979 Computational aerodynamics development and outlook. *AIAA J.* **17** 1293.

GEORGE, W. K., BEUTHER, P. D. & ARNDT, R. E. A. 1984 Pressure spectra in turbulent free shear flows. *J. Fluid Mech.* **148**, 155-191.

GHOSAL, S., LUND, T. S., MOIN. P. & AKSELVOLL, K. 1994 A localization model for large-eddy simulation of turbulent flows. Submitted to *J. Fluid Mech.*

JIMÉNEZ, J., WRAY, A., SAFFMAN, P. G. & ROGALLO, R. S. 1993 The structure of intense vorticity in homogeneous isotropic turbulence. *J.Fluid Mech.* **255** 65-90.

KERR, R. M. 1985 Higher-order derivative correlations and the alignment of small-scale structures in isotropic numerical turbulence. *J. Fluid Mech.* **153**, 31-58.

KERR, R. M., 1990 Velocity, scalar and transfer spectra in numerical turbulence. *J. Fluid Mech.* **211**, 309-322.

LUNDGREN, T. S. 1982 Strained spiral vortex model for turbulent fine structure. *Phys Fluids* **25**, 2193-2203.

OBUKHOV, A. M. 1949 Pressure fluctuations in a turbulent flow *Dokl. Akad, Nauk SSSR, Ser. Geofiz.* **3**, 49-68.

PULLIN, D. I. 1994 Pressure spectra for vortex models of fine-scale homogeneous turbulence. *Phys Fluids* (in press).

PULLIN, D. I., BUNTINE, J. D. & SAFFMAN P. G. 1994 On the spectrum of a stretched spiral vortex. *Phys Fluids* **6**, 3010.

PUMIR, A. 1994 A numerical study of pressure fluctuations in three-dimensional, incompressible, homogeneous, isotropic turbulence. *Phys Fluids* **6** 2071.

SHE, Z.-S. & JACKSON, E. 1993 A constrained Euler system for Navier-Stokes turbulence. *Phys. Rev. Lett.* **70** 1255.

TSINOBER, A., KITT, E. & DRACOS, T. 1992 Experimental investigation of the field of velocity gradients in turbulent flows. *J. Fluid Mech.* **242** 169.

SADDOUGHI, S. G. & VEERAVALLI, S. V. 1994 Local isotropy in turbulent boundary layers at high Reynolds number. *J. Fluid Mech.* **268**, 333.